HHS Public Access

Author manuscript

Biomater Sci. Author manuscript; available in PMC 2024 August 08.

Published in final edited form as:

Biomater Sci. ; 11(16): 5641–5652. doi:10.1039/d3bm00627a.

Polymer/copper nanocomplex-induced lysosomal cell death promotes tumor lymphocyte infiltration and synergizes anti-PD-L1 immunotherapy for triple-negative breast cancer

Xiangxiang Hu[a], **Mingming Wang**[a], **Shanshan Shi**[a], **Manikanda Keerthi Raja**[b], **Gourab Gupta**[b], **Hexin Chen**[b], **Peisheng Xu**[a]

[a]Department of Drug Discovery and Biomedical Sciences, University of South Carolina,715 Sumter St. Columbia, SC 29208, United States.

[b]Department of Biological Sciences, University of South Carolina, 715 Sumter St. Columbia, SC 29208, United States.

Abstract

Our previous research discovered that combining PDA-PEG polymer with copper ions can selectively kill cancer cells. However, the precise mechanism by which this combination function was not fully understood. This study revealed that PDA-PEG polymer and copper ions form complementary PDA-PEG/copper (Poly/Cu) nanocomplexes by facilitating copper ion uptake and lysosomal escaping. *In vitro* study found that Poly/Cu killed 4T1 cells through a lysosome cell death pathway. Furthermore, Poly/Cu inhibited both proteasome function and autophagy pathway and induced immunogenic cell death (ICD) in 4T1 cells. The Poly/Cu induced-ICD coupled with the checkpoint blockade effect of anti-PD-L1 antibody (aPD-L1) synergistically promoted immune cells penetration into the tumor mass. Benefiting from the tumor-targeting effect and cancer cell-selective killing effect of Poly/Cu complexes, the combinatory treatment of aPD-L1 and Poly/Cu effectively suppressed the progression of triple-negative breast cancer without inducing systemic side effects.

Graphical Abstract:

xup@cop.sc.edu; Fax: 803-777-8356; Tel: 803-777-0075.

Author contributions

Methodology, formal analysis, investigation, writing – original draft, and visualization, X.H.; methodology and investigation, M.W.; methodology and investigation, S.S.; methodology and investigation, M.R.; methodology and investigation, G.G.; methodology and resources, H.C.; conceptualization, methodology, resources, writing – review and editing, supervision, P.X.; all authors have read and agreed to the published version of the manuscript.

Declaration of Competing Interests:

The authors declare that they have no known competing financial interests to influence the work reported in this paper.

[†]Electronic Supplementary Information (ESI) available. See DOI: 10.1039/x0xx00000x

Supporting Information

Supplementary material associated with this article can be found in the online version.

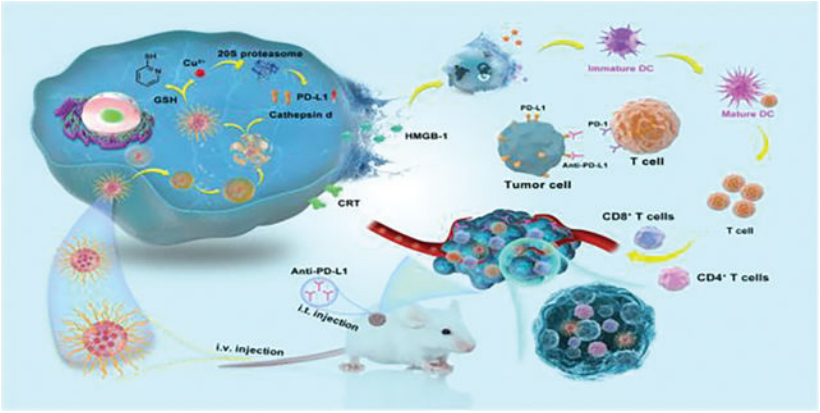

PDA-PEG/copper nanocomplex kills 4T1 cells by lysosomal cell death, and exhibts synergetic effect with PD-L1 antibody through ICD-boosted T-cell infiltration.

Introduction

Chemotherapy has been a widely used approach in treating breast cancer, but the non-specific toxicity of the drugs can result in serious side effects for patients.[1, 2] In the meantime, checkpoint blockade-based immunotherapies targeting T-cells have attracted significant attention. One such example is the use of programmed death-ligand 1 (PD-L1) antibody,[3–6] which has shown promising results in clinical trials and has even been approved by the FDA for the treatment of various types of cancer.[7, 8] However, recent studies revealed that the efficacy of the anti-PD-L1 antibody (aPD-L1) could be limited in some patients due to a lack of T-cell infiltration into the tumor mass. This has been referred to by some as a "cold tumor" phenomenon.[9, 10]

Improving the effectiveness of cancer immunotherapy requires converting a "cold tumor" into a "hot tumor" that has a high concentration of immune cells.[11, 12] To overcome this challenge, researchers are exploring combination treatments, such as combining chemotherapy with checkpoint blockade immunotherapy, to achieve a stronger antitumor effect.[13] These efforts are being aided by the use of immunogenic cell death (ICD), which helps immune cells infiltrate into the tumor mass.[14, 15] However, conventional anticancer drugs have off-target effects and can cause significant side effects, presenting a major obstacle to overcome.

Our group previously developed poly [(2-(pyridin-2-yldisulfanyl) ethyl acrylate)-co- [poly (ethylene glycol)]] (PDA-PEG) for cancer-targeted drug delivery.[16] A recent study found that PDA-PEG can form nanocomplexes with copper ions (Poly/Cu) in the aqueous phase and exhibit a cancer cell-selective killing effect.[17] However, the mechanism of Poly/Cu toxicity in breast cancer is unclear. Herein, we adopted 4T1 cells-based triple-negative breast cancer (TNBC) model to study the mechanism of Poly/Cu toxicity. It was revealed that Poly/Cu induced lysosomal cell death, inhibited proteasome function, and promoted PD-L1 expression. More importantly, Poly/Cu also induced ICD on the 4T1 cells, which would further increase the immune response. To take advantage of the Poly/Cu induced ICD and

inhibit the upregulated PD-L1 interacting with PD-1 with T cells, aPD-L1 was incorporated to probe the potential synergy of the ICD effect of Poly/Cu and the checkpoint blockade effect of aPD-L1 for TNBC therapy (Fig. 1A).

Results

Characterization of Poly/Cu

The PDA-PEG polymer (Poly) was synthesized according to the previous report.[16] The polymer has both hydrophobic segments, 2-(pyridin-2-yldisulfanyl) ethyl acrylate, and hydrophilic segments, poly (ethylene glycol). By taking advantage of this property, Poly/Cu nanocomplexes were fabricated by dissolving the polymer into water and mixing it with a copper chloride solution. Dynamic light scattering found the size of the resulting nanocomplexes in the water was about 30 nm (Fig. 1B), which matched with transmission electron microscopy observation. The PDI of nanocomplexes is 0.25, indicating the narrow size distribution. Furthermore, the stability assay proved that the size of the nanocomplexes remained constant over seven days in phosphate-buffered saline (PBS) (Fig. 1C). In addition, the size of the nanocomplexes in 10% FBS containing buffer exhibited no significant difference within 24 h, suggesting the excellent biocompatibility of Poly/Cu with blood components during circulation. (Fig. 1D).

Poly/Cu killing of 4T1 cells is copper-dependent

Copper ions are essential in cancer progression and metastasis, involving mitochondria breathing, anti-oxidation, and signal pathways.[18–20] Thus, many explored anticancer therapies have focused on disrupting copper homeostasis by manipulating copper ion level within cancer cells.[21–23] Our previous study revealed that PDA-PEG polymer or copper alone has less toxicity to the tumor cells, while their combination exhibits highly selective toxicity to cancer cells over normal cells.[17] However, the mechanism for PDA-Poly/Cu nanocomplexes selectively killing cancer cells was unclear. To address that, TNBC 4T1 cells were adopted. For the combination of PDA-PEG and Cu ions, the increase of PDA-PEG concentration or copper ion concentration resulted in the increase of their cytotoxicity (Fig. 2A, 2B), which proved that Poly/Cu toxicity is dose-dependent. As expected, PDA-PEG or copper ions alone did not induce significant toxicity (Fig. S1A), suggesting only the combination of PDA-PEG and Cu could generate toxicity in the 4T1 cells. To investigate the effect of PDA-PEG on intracellular copper ion level, Phen Green™ FL diacetate, a copper ion selective dye, was employed. It was revealed that the addition of Cu moderately increases the intracellular copper concentration. Similarly, the addition of PDA-PEG alone only slightly affects the copper ion concentration in the 4T1 cells (Fig. 2C and Fig. S1B). Interestingly, the treatment of Poly/Cu combination effectively quenched the intracellular fluorescence signal, suggesting that PDA-PEG could deliver a significantly higher level of copper ions into the 4T1 cells than $CuCl_2$ alone. Thus, we hypothesize that PDA-PEG may form nanoparticles and deliver more copper ions into 4T1 cells and induce the death of these cells. To further validate the effect of intracellular copper ions on the cytotoxicity of PDA-PEG, ammonium tetrathiomolybdate (TTM), a copper chelator, was introduced. TTM treatment reduced intracellular copper ion level, evidenced by the enhanced green fluorescence intensity (Fig. 2D). To reduce the intracellular copper ion

level, TTM was added together with the Poly/Cu treatment. As expected, the addition of TTM reduced the copper ions within the cells (Fig. 2D and Fig. S1C) and attenuated the cytotoxicity of Poly/Cu on 4T1 cells (Fig. 2E and Fig. S1D). In contrast, no noticeable fluorescence intensity change was observed in NIH-3T3 cells after copper ions and Poly/Cu treatment, indicating the combinatory treatment of PDA-PEG and Cu could not increase the intracellular copper level in NIH-3T3 cells (Fig. S2A–B). Consequently, Poly/Cu could not effectively kill NIH-3T3 cells (Fig. S2C). Thus, Poly/Cu exhibited selective toxicity on tumor cells while sparing normal cells (NIH 3T3). All the above data suggested that a high level of intracellular copper ions is critical for killing 4T1 cells. At the same time, PDA-PEG may form nanoparticles and deliver copper ions into tumor cells and cause tumor cell death.

Poly/Cu induces lysosomal cell death

Our study found that PDA-PEG forms nanoparticles in an aqueous solution, and the nanoparticles could be endocytosed to the endosome and then transferred to the lysosome. To escape from the lysosome, nanoparticles usually break the lysosome and get released into the cytoplasm due to a proton sponge effect, especially with the help of copper ions.[24, 25] PDA-PEG can effectively enter 4T1 cells and accumulate in their lysosomes. At the same time, the addition of copper ions did not boost the uptake of PDA-PEG by the 4T1 cells (Fig. 3A), which coincides with our previous observation in SKOV-3 cells.[17] Interestingly, it was noticed that the combinatory treatment of PDA-PEG and Cu ions induced the enlargement of the lysosome (Fig. 3B). Moreover, their combination significantly reduced the number of lysosomes in the 4T1 cells. Thus, we postulate that Poly/Cu may induce lysosomal cell death (LCD) by breaking lysosomes and releasing the lysosomal content into the cytoplasm.[26, 27] Acridine orange is a lysosomotropic agent, which emits a red fluorescence when retained within lysosomes at a high concentration and yields green fluorescence signals when localized in cytosol at a low concentration. To further test the above hypothesis, the permeability of lysosomes in 4T1 cells was analyzed by acridine orange staining. It was found that after 12 h of treatment, Poly/Cu significantly increased the permeability of lysosome in the 4T1 cells, evidenced by the elevated green:red fluorescence ratio (Fig. 3C and Fig. S3A). As expected, PDA-PEG or Cu alone did not affect the lysosomal permeability.

Cathepsin D is a lysosomal protease,[28] that can be released into the cytoplasm when the lysosome is broken. To further prove that Poly/Cu broke lysosomes, the distribution of cathepsin D in 4T1 cells was determined by immunofluorescence staining. The smeared red signals in Fig. 3D confirmed that Poly/Cu promoted the release of cathepsin D into the cytoplasm, indicating that Poly/Cu facilitated the rupture of the lysosomes in 4T1 cells.

Additionally, Poly/Cu didn’t induce reactive oxygen species (ROS) elevation (Fig. 3E and Fig. S3B). Western blot results found that Poly/Cu did not induce the expression of cleaved-PARP and cleaved-caspase 3 (Fig. 3F–G and Fig. S3C–D), which are the hallmarks of apoptosis. These data collectively proved that Poly/Cu results in the enlargement of the lysosome, increases the permeability of lysosomes, breaks the lysosome, and causes lysosomal cell death of 4T1 cells.

Poly/Cu inhibits proteasome function and prevents the degradation of PD-L1

PDA-PEG facilitates the uptake of copper ions by cancer cells and subsequently kills them, similar to a disulfiram (DSF)/copper complex in killing cancer cells.[29, 30] One of the main targets of the DSF/copper complex is the ubiquitin/proteasome system (UPS).[31] The ubiquitin/proteasome system is a highly regulated mechanism for intracellular protein degradation, which plays an essential role in many fundamental cellular activities.[32, 33] A protein must be ubiquitinated before it can be transferred to the 26S proteasome system for degradation. As demonstrated in Fig. 4A–B, Poly/Cu boosted the expression of poly-ubiquitin protein, indicating that Poly/Cu inhibited the function of proteasome and caused the accumulation of ubiquitinated protein. The 26S proteasome system comprises a catalytic core particle (also known as 20S proteasome) and one or two 19S regulatory particles.[34] To better understand the mechanism of proteasome inhibition by Poly/Cu, the activity of 20S proteasome was analyzed. 4T1 cells were treated with different concentrations of copper ions, PDA-PEG polymer, and their combinations for 24 h. After that, 20S proteasome from the 4T1 cells was isolated, and the activity of 20S proteasome was analyzed. As expected, polymer or copper ion alone has no significant influence on the activity of 20S proteasome (Fig. 4C–D), while their combination showed an inhibitory effect on the 20S proteasome function (Fig. 4E). In another set of experiments, 20S proteasomes were isolated from untreated cells first and then treated with different concentrations of PDA-PEG polymer, copper ion, and their combination. In agreement with a previous report,[35] free copper ions alone produced a significant suppression effect on the function of 20S proteasome (Fig. S4B). Interestingly, Poly/Cu only showed a weak inhibitory effect on 20S proteasome, which might be due to PDA-PEG polymer's chelator effect subsequently reducing the free copper ions level in the system. Taken together, we conclude that the enhanced 20S proteasome inhibitory effect of Poly/Cu was because PDA-PEG facilitated the intracellular uptake of copper ions.

Many researchers reported that UPS-proteasome is a primary pathway to degrade programmed death-ligand 1(PD-L1).[36, 37] Fig. 4F and Fig. S4D–E revealed that Poly/Cu also suppressed the degradation of PD-L1, evidenced by the increased PD-L1 expression in PDA-PEG/copper treated cells, which is similar to that resulted from the treatment of bortezomib (BTZ), a proteasome inhibitor (Fig. 4G–H and Fig. S4F–G). Therefore, Poly/Cu-induced proteasome inhibition also induced the overexpression of PD-L1 in 4T1 cells, which potentially may result in immunosuppression in cancer therapy.

Poly/Cu inhibits autophagy in 4T1 cells

Since the fusion of lysosomes with autophagosomes to form autolysosomes is required during the autophagy process,[38] the break of lysosomes by Poly/Cu treatment would inhibit the function of autophagy. Thus, LC3B-II, an autophagy marker, would not be degraded by the autolysosomes when the upstream lysosome was broken. To validate our hypothesis, Cyto-ID was utilized to detect the expression of LC3B-II. Rapamycin, an inhibitor of the mTOR signal and inducer of autophagy, was adopted as a positive control. It was found that the Poly/Cu treatment upregulated LC3B-II expression (Fig. 5A). Western blot results further proved that LC3B-II expression was increased by Poly/Cu (Fig. 5B–C). These data demonstrated that Poly/Cu inhibited the autophagy of 4T1 cells.

Ubiquitin-proteasome and autophagy-lysosome are two major pathways for intracellular protein degradation, as previous studies demonstrated.[39–43] To probe the relationship between autophagy and proteasome activities in 4T1 cells upon Poly/Cu treatment, rapamycin (autophagy promotor) and chloroquine (CQ, autophagy inhibitor) were introduced. Fig. 5C and Fig. 5E verified that both rapamycin and CQ alone or in combination with Poly/Cu increased the expression of LC3B-II. However, rapamycin could reduce the Poly/Cu upregulated poly-ubiquitin expression (Fig. 5D and Fig. S5C), while CQ further increased the expression of poly-ubiquitin induced by Poly/Cu (Fig. 5F and Fig. S5D). Thus, we concluded that the autophagy suppression effect of Poly/Cu further boosted its proteasome inhibitory effect in 4T1 cells.

PDA-PEG/copper induces immunogenic cell death

Immunogenic cell death (ICD) is a type of cell death that promotes immune response. Calreticulin (CRT) translocating to the membrane and releasing high mobility group box 1 (HMGB1) are two major makers of ICD[44]. Some studies have reported that heat shock protein 70 (HSP70) upregulation also increases tumor immunogenicity.[45] PDA-PEG/copper has been found to selectively kill tumor cells by inducing lysosomal cell death (Fig. 3). It was interesting to see that Poly/Cu treatment helps the translocation of CRT to the cell membrane (Fig. 6A–B), which promoted dead cell-associated antigen uptake by dendric cells (DCs). Moreover, Poly/Cu treatment decreased the concentration of HMGB1 in the 4T1 cells, suggesting that Poly/Cu encouraged the release of HMGB1 (Fig. 6C–D), which subsequently favored the recruitment of DCs and their activation. Additionally, Poly/Cu treatment also significantly increased the expression of HSP70 (Fig. 6E–F). All these data proved that PDA-PEG/copper induced ICD on 4T1 cells.

aPD-L1 boosts the cell-killing effect of Poly/Cu *in vitro*

Poly/Cu inhibits the function of proteasome and results in the accumulation of PD-L1, which is related to immune escape and poor prognosis.[46, 47] To boost the therapeutic effect of Poly/Cu and reduce its associated immune suppression for cancer therapy, aPD-L1, which blocks the interaction between cancer cells expressed PD-L1 and T cells expressed PD-1, was introduced. Fig. 7A found that Poly/Cu killed nearly 60% of 4T1 cells, while the addition of aPD-L1 boosted its cytotoxicity by 10%. In contrast, aPD-L1 itself had no significant toxicity on 4T1 cells *in vitro* (Fig. 7A, 7C). To mimic the *in vivo* situation *in vitro*, we co-cultured peripheral blood mononuclear cells (PBMCs) and aPD-L1 with 4T1 cells for five days after 4T1 cells were pretreated with Poly/Cu for 2 days. In the non-pretreated group, it was discovered that PBMCs or aPD-L1 alone did not kill 4T1 cells, and their combination only exhibited slight toxicity (Fig. 7B and 7D). However, for the Poly/Cu pretreated group (Fig. 7B and 7E), the supplement of PBMCs killed nearly an additional 30% of cells, and the combination of aPD-L1 and PBMCs caused an additional 40% of 4T1 cell death. We postulate the enhanced cell-killing effect of the combination of aPD-L1 and PBMCs was due to the ICD induced by Poly/Cu (Fig. 6), which promoted the attack of cytolytic T cells in killing 4T1 cells. Besides that, PD-L1 inhibition with the help of the aPD-L1 further boosted the activity of the cytolytic T cells.

To further validate the system in a more *in vivo* relevant model, 4T1 tumor spheroids were created and treated similarly as described in 2D culture. Fig. S6 showed that there were only a few dead 4T1 cells in aPD-L1 or PBMCs-treated groups when the 4T1 tumor spheroids were not pretreated with Poly/Cu. However, when 4T1 tumor spheroids were pretreated with Poly/Cu, PBMCs induced significant damage to 4T1 tumor spheroids. This enhanced killing effect was more significant when aPD-L1 and PBMCs combinatory treatment was given. Therefore, we expected that the combinatory treatment of Poly/Cu and aPD-L1 should effectively inhibit tumor growth *in vivo*.

In vivo distribution of Poly/Cu

Encouraged by the excellent *in vitro* results, we further studied the tumor-targeting effect of Poly/Cu. A mouse xenograft tumor model was built by injecting 4T1 cells subcutaneously. The *in vivo* distribution of cy5-labeled PDA-PEG or PDA-PEG/copper in the mouse tumor model was studied by an IVIS animal imaging system. It was revealed that PDA-PEG nanoparticles were mainly distributed to the liver, lung, and kidney (Fig. S7). Interestingly, the addition of copper ions improved the retention of PDA-PEG nanoparticles in tumor tissue.

In vivo antitumor effect of combinatory treatment

To investigate the antitumor effect of Poly/Cu combined with aPD-L1 *in vivo*, 4T1 tumor-bearing BALB/c mice were assigned to four treatment groups, including control, aPD-L1, Poly/Cu, and the combination of aPD-L1 and Poly/Cu, and being treated as described in Fig. 8A when tumor volume reached 50 mm^3. To generate stronger checkpoint blockage effect and minimize potential systemic toxicity of aPD-L1, intratumor injection of aPD-L1 was employed. Fig. 8B and 8E indicated that the tumor volume in the control group increased rapidly, reaching 2000 mm^3 in less than 30 days. As expected, the intratumor injection of aPD-L1 only slightly inhibited the growth of the tumor (Fig. 8B and 8F). At the same time, the treatment of Poly/Cu exhibited a significant inhibitory effect (Fig. 8B and 8G). To our surprise, the combination of aPD-L1 and Poly/Cu showed a much more potent effect in inhibiting tumor progression than aPD-L1 or Poly/Cu alone (Fig. 8B and 8H). Benefiting from its remarkable anticancer effect, the medium survival time for the combination treatment group was extended from 28 days to 53 days (Fig. 8C). In the meantime, no significant weight change (Fig. 8D) and tissue damage (Fig. S8) were noticed among all treatment groups, suggesting the safety of the combinatory treatment.

To probe whether the ICD effect of Poly/Cu combined with aPD-L1 induced the infiltration of T cells *in vivo*, immunohistochemistry was employed to detect the residence of the T cells within the tumor tissue. Fig. 8I–K revealed that aPD-L1 or Poly/Cu alone did not induce the infiltration of $CD3^+$, $CD4^+$, and $CD8^+$ cells within the tumor tissue. However, as expected, the combinatory treatment of aPD-L1 and Poly/Cu effectively promoted the $CD3^+$, $CD4^+$, and $CD8^+$ cells' penetration into the tumor mass. Furthermore, Ki67 immunostaining revealed that the cancer cells within the combinatory treatment group had the slowest growth rate (Fig. 8L). All these data proved that the aPD-L1 exhibited a synergetic effect with the ICD effect of Poly/Cu in promoting immune cell infiltration into tumor mass, which

subsequently enhanced the antitumor effect of Poly/Cu and prolonged the survival time of mice.

Discussion

Intracellular copper ions are critical for the proliferation of cancer cells. However, a high level of copper ions in the cytoplasm inhibits the activity of the proteasome. Our study revealed that PDA-PEG polymer and copper ions were mutually reinforced after forming polymer/metal nanocomplex (Fig. 1B). PDA-PEG helped copper ions enter the cancer cells (Fig. 2C) while copper ions assisted PDA-PEG escaping from the lysosome (Fig. 3). Due to their complementary effect, Poly/Cu selectively killed cancer cells by boosting the permeability of the lysosome (Fig. 1), causing the rupture of the lysosomes and the release of cathepsin enzymes to kill cancer cells (Fig. 3). Moreover, Poly/Cu inhibited the proteasome function by suppressing the 20S proteasome function (Fig. 4A–E) as well as preventing the degradation of PD-L1, which resulted in the upregulation of PD-L1 (Fig. 4F). Because of the breaking of lysosomes, Poly/Cu also inhibited the autophagy pathway (Fig. 5). Autophagy and proteasome system are two major pathways for intracellular protein degradation. Usually, proteasome inhibition may promote the autophagy-based protein degradation pathway. Interestingly, Poly/Cu blocked both proteasome and autophagy pathways simultaneously. In addition, Poly/Cu induced ICD for 4T1 cells, evidenced by the increased CRT membrane translocation and declined intracellular HMGB1 level (Fig. 6), which subsequently promoted an immune response. Based on the above results, we introduced aPD-L1 to Poly/Cu treatment to achieve a better antitumor effect for TNBC. It was revealed that aPD-L1 increases the antitumor effect of Poly/Cu in 2D and tumor spheroid culture, especially in the presence of PBMCs (Fig. 7 and Fig. S6). During the *in vivo* study, aPD-L1 based PD-L1 inhibition and Poly/Cu induced ICD boosted the infiltration of immune cells into tumor mass (Fig. 8I–J), synergistically killed 4T1 cancer cells (Fig. 8A), prevented the progression of tumor (Fig. 8B), and prolonged the survival time of the animals (Fig. 8C). Ascribed to the cancer cell-selective killing nature of Poly/Cu, no systemic toxicity was observed after the combinatory treatment of aPD-L1 and Poly/Cu.

Experimental section

Materials

Ki67-Alexa 488, Cleaved-PARP, LC3B, Poly-ubiquitin, and HSP70 antibodies were purchased from the Cell signaling technique, Inc. PD-L1 monoclonal antibody (aPD-L1) was obtained from Bio X Cell. CD3, CD4, and CD8 antibodies were purchased from Protein Techniques, Co. Cyanine5 NHS ester was purchased from Lumiprobe Corporation. Ammonium tetrathiomolybdate, ROS Kit (H2DCF-DA), Cupric chloride, and copper gluconate were purchased from Sigma-Aldrich. 3-[4,5-Dimethylthiazol-2-yl]-2,5-diphenyltetra-zoliumbromide (MTT), Phen Green™ FL Diacetate dye, fetal bovine serum (FBS), 0.25% trypsin-EDTA, penicillin-streptomycin (PS), phosphate-buffered saline (PBS), DAPI, calcein AM, ethidium Homodimer-1 (EthD-1), Alexa fluor 633 goat anti-rabbit IgG, and Alexa fluor 488 goat anti-mouse IgG were purchased from Thermo Fisher Scientific, Inc. Cyto-ID kit was purchased from Enzo Life Sciences, Inc. Suc-LLVT-AMC, Ac-RLR-

AMC, and Z-LLE-AMC were purchased from Cayman Chemical, Co. All the solvents used in this study were bought from Sigma-Aldrich Chemical Co. (St. Louis, MO, USA) and used directly without further purification unless specified.

Fabrication of Poly/Cu nanocomplexes

PDA-PEG polymer was synthesized according to a previous study.[16] To fabricate Poly/Cu nanocomplexes, briefly, 10 mg Polymer was dissolved into 10 ml DI water and sonicated for 10 min, 5 μL 20 mM copper ions were added into the above solution. The size of Poly/Cu nanocomplexes was detected by dynamic light scattering (DLS, Zetasizer Nano ZS, Malvern Instruments Ltd, Malvern, UK). The morphology of Poly/Cu nanocomplexes was studied by Hitachi HT7800 transmission electron microscopy (TEM, Hitachi High-Technologies Corporation, Tokyo, Japan).

Stability of Polymer/copper

The hydrodynamic stability of the Poly/Cu nanocomplexes was monitored by DLS. Nanogels were first dispersed in PBS buffer (pH 7.4) for 7 days, and the size of the nanoparticles was determined with DLS every day. Poly/Cu nanocomplexes were incubated in the PBS buffer with 10% FBS (pH 7.4) at 37 °C for 24 h, and the size of the nanocomplexes was determined with DLS at predetermined time points.

MTT assay

4T1 breast cancer cells were cultured in Gibco™ DMEM supplemented with 10% FBS, 100 units/mL of penicillin, and 100 μg/mL of streptomycin at 37 °C with 5% CO_2 under a humidified atmosphere. Cells were seeded in a 96-well plate at the density of 3000 cells/well and incubated overnight. After that, different concentrations of PDA-PEG combined with 10 μM copper ions ($CuCl_2$) or other indicated concentrations of drugs were added into culture media and incubated for another 48 h. After removing the old medium, MTT reagent was added to the 96-well plate with fresh medium and incubated for another 4 h or until purple crystal formed. After that, the medium was replaced with 200 μL DMSO. Cell viability was analyzed by recording the absorbance of each well at 570 nm with a microplate reader.

ROS assay

4T1 cells were seeded in a black 96-well plate at the density of 3000 cells/well and incubated overnight. After that, different concentrations of PDA-PEG combined with 10 μM copper ions ($CuCl_2$) were added to the culture media and incubated for another 12 h. Ten μM H2DCF-DA was added into each well and incubated for another 30 min. After that, the medium was removed, and cells were washed with cold PBS. The ROS in the 4T1 cells were imaged by the Carl Zeiss LSM700 confocal microscope and quantified by the microplate reader.

Copper uptake

4T1 cells were seeded in a glass-bottom dish for overnight culture, then indicated treatments were added into the culture medium for 6 h. The old medium was replaced with fresh medium containing Phen green™ dye and incubated for another 30 min. 4T1 cells were

washed with PBS buffer 3 times, and the copper concentration in the 4T1 cells was detected by a Carl Zeiss LSM700 confocal microscope.

Cellular Internalization assay

4T1 cells were seeded in 35 mm glass-bottom dishes at a density of 4×10^4 cells per well. After 24 h of incubation at 37 °C, the old medium was replaced with a fresh medium containing 10 μM Poly-Cy3 or 10 μM Poly-Cy3 combined with 10 μM Cu. After incubating for 4 h, cells were washed with PBS and fixed with 4% paraformaldehyde (PFA) for 15 min. Finally, the nuclei were stained with 10 μg/ml of DAPI for 10 min at room temperature. The uptake of PDA-PEG was observed with a Carl Zeiss LSM700 confocal microscope.

Acridine orange staining assay

4T1 cells were seeded in a glass bottom dish for overnight culture, then 4T1 cells were incubated with 20 μM PDA-PEG, 10 μM $CuCl_2$, and their combination for 24 h. The old medium was replaced with fresh medium containing 10 μM Acridine orange for 15 min, then 4T1 cells were washed with PBS 3 times. The permeability of the lysosome was determined by Carl Zeiss LSM700 confocal microscope.

Western blot assay

4T1 cells were seeded into a 6-well plate at the density of 14×10^4 cells/well. After overnight culture, different concentrations of PDA-PEG combined with 10 μM $CuCl_2$ or other indicated concentrations of drugs were added into the media, and the cells were incubated for another 48 h. Afterward, 4T1 cells were harvested and lysed, and the concentrations of proteins were determined by a BCA protein assay. Proteins were separated in an SDS-PAGE gel and transferred to a PVDF membrane. After the membrane was blocked with 3% BSA for 1 h, it was incubated with different primary antibodies (HMGB-1, HSP70, LC3B, PARP, Poly-ubiquitin, PD-L1) overnight at 4 °C, washed with BST buffer for 3 times, incubated with secondary antibody for 2 h at room temperature, and then imaged with the help of enhanced chemiluminescence to detect the targeted protein expression.

Autophagy staining assay

4T1 cells were seeded in a glass-bottom dish and received different treatments for 24 h. The old medium was removed, and 4T1 cells were washed with PBS and fixated with 4% PFA. Then 4T1 cells were incubated with DAPI and Cyto-ID for 30 mins at 37 °C before being imaged with a Carl Zeiss LSM700 confocal microscope.

20S proteasome activity assay

To measure the proteasome activity in 4T1 cells, 4T1 cells were seeded into 6-well plates. After 12 h of culture, cells were incubated with different concentrations of PDA-PEG, varying concentrations of $CuCl_2$, or their combination for 48 h. Cells were washed twice with ice-cold PBS and then collected with an isolating buffer (50 mM HEPES (pH 7.5), 150 mM NaCl, 1% Triton X-100, and 0.1 μM PMSF) and then centrifuged at 15,000 rpm for 15 min at 4°C. The cell lysates (10 μg) were incubated with 20 μM of different substrates (Suc-LLVT-AMC, Ac-RLR-AMC, and Z-LLE-AMC) for measurement of chymotrypsin-

like (CT like), trypsin-like (T like), and caspase-like (C like) activities, respectively. After 2 h of incubation at 37 °C, proteasome activity was measured by the release of hydrolyzed free AMC groups by microplate reader at 380/460 nm. To measure the 20S proteasomes activity of untreated 4T1 cells in response to drug treatment, 20S proteasomes isolated from the untreated 4T1 cells were incubated with 20 μM of different substrates to measure chymotrypsin-like, trypsin-like, and caspase-like activities in assay buffer (30 mM Tris-HCl (pH 7.4)) with different concentrations of PDA-PEG, varying concentrations of $CuCl_2$, or their combination. After 2 h of incubation at 37°C, the proteasome enzymatic activities were measured by the release of hydrolyzed free AMC as described above.

Immunofluorescence staining

For cell immunofluorescence staining assay, 4T1 cells were seeded in a glass-bottom dish and treated with the drugs described above for 48 h. After that, the cells were washed with PBS, fixated by 4% PFA, and incubated with 3% BSA for 1 h at room temperature. The primary antibody was added to the dish overnight at 4°C. The secondary antibody (goat anti-rabbit-cy5 or goat anti-mouse Alexa 488) was added to the dish for 1 h at room temperature. The expression of the indicated protein was imaged by the confocal microscope (Carl Zeiss LSM700). For the tissue immunofluorescence staining, the OTC-embedded tissue sections were blocked in 5% BSA for 1 h at room temperature. Slides were incubated with primary antibodies overnight at 4 °C and incubated with fluorescence-labeled secondary antibodies at 37 °C for 1 h. Finally, the slides were mounted with Prolong® Diamond Antifade Mounting with DAPI. Immunofluorescence images of the tissues were recorded with a confocal microscope.

Flow cytometry assay

To investigate the effect of PDA-PEG/copper on the expression of CRT, flow cytometry was employed. Cells were incubated with PDA-PEG/copper for 48 h and collected after trypsinization. Cells were fixated by 4% PFA, washed with PBS buffer, and incubated with 3% BSA for 1 h at room temperature. The CRT antibody (1:2000) solution was added to the cells overnight at 4°C. The secondary antibody (goat anti-rabbit-cy5) was incubated with the cells for 1 h at room temperature. The concentration of CRT on the 4T1 cells membrane after PDA-PEG/copper treatment was determined by flow cytometry (BD Accuri C6, BD Biosciences).

Tumor spheroid assay

4T1 cells were seeded in a Corning Ultra-Low Attachment 96-well plate (4,000 cells/well). After 4 days of incubation or till the formation of tumor spheroids, tumor spheroids were pretreated with 20 μM PDA-PEG/10 μM $CuCl_2$ for 2 days. Afterward, the old medium was replaced with fresh medium containing PBMCs (Effector/Target=30) and/or aPD-L1 (50 μg/ml) and their combination for 2 days. The viability of the cells in the tumor spheroid was detected by staining with calcein AM and ethidium Homodimer-1 (EthD-1) dye.

In vivo distribution of Poly/Cu

All animal procedures were performed in accordance with the Guidelines for Care and Use of Laboratory Animals of the University of South Carolina and approved by the Institutional Animal Care and Use Committee (IACUC) (2570-101653-093021). BALB/c mice were purchased from Jackson Laboratory. The xenograft breast cancer model was established by subcutaneously injecting 4T1 cells (2×10^5 cells in 200 μL PBS) into the back of the mice body of 6-week-old mice. Two weeks after the inoculation of 4T1 cells, the mice were intravenously administered the Poly-Cy5 or Poly-Cy5/Cu as the treatment group while injected PBS as the control. Three hours post-injection, mice were sacrificed, and different organs and tumor masses were collected to be imaged *ex vivo* by an IVIS Lumina III whole-body imaging system.

Anti-tumor efficacy

Tumor-bearing mice established above were randomly assigned into 4 groups (n=5) when the tumor volume (V=Length* width^2/2) reached 50 mm^3, and injected with 1) PBS (i.v.), 2) aPD-L1 (intratumorally injection, 50 μg per mice), 3) Poly/Cu (i.v., 80 mg/kg Poly, 3.57 mg/kg copper gluconate), 4) the combination treatment of 2) + 3). To reduce the risk of immune overreaction of PD-L1 antibody, only three doses of aPD-L1 treatment were administered in treatment group 2) and 4). Animals in treatment groups 3) and 4) received 8 doses of Poly/Cu (twice per week). The sizes of the tumors were recorded twice per week for 70 days or until tumor volume reached 2000 mm^3.

Histological analysis

The organs collected from different treatment groups were fixed in the 4% paraformaldehyde solution at 4 °C for 24 h, then embedded in optimal cutting temperature compound (OCT compound). The embedded organs were cut into sections of 12 μm thickness. Afterward, the tissue sections were stained with Hematoxylin and eosin (H&E) and analyzed under a light microscope.

Statistical analysis

All data were processed and expressed as means with standard deviations (mean ± SD). All experiments were repeated at least three times. Student's t-test was utilized to analyze the statistical difference between parallel groups. $P < 0.05$ from a two-tailed test was considered statistically significant.

Conclusions

In summary, we discovered that PDA-PEG/copper nanocomplexes could kill 4T1 cells through a lysosomal cell death pathway, in which PDA-PEG and copper ions are complementary in promoting the intracellular copper ion level and facilitating lysosomal escaping. Poly/Cu blocks both the proteasome function and autophagy pathway, leading to PD-L1 overexpression. To counteract the potential immune suppression effect of upregulated PD-L1, aPD-L1 was coupled with the Poly/Cu treatment. The synergistic effects of Poly/Cu induced ICD and aPD-L1's checkpoint blockade promote immune cell infiltration into the tumor and kill cancer cells. Benefiting from the tumor-targeting effect and cancer cell-

selective killing effect of Poly/Cu nanocomplexes, the combinatory treatment of aPD-L1 and Poly/Cu effectively inhibits the progression of TNBC without inducing systemic toxicity effects.

Supplementary Material

Refer to Web version on PubMed Central for supplementary material.

Acknowledgments

The authors want to thank the National Institutes of Health (1R01CA263747-01A1 and 1R21CA252360-01) for the financial support of the research.

References

1. Yan L, Shen J, Wang J, Yang X, Dong S and Lu S, Dose Response, 2020, 18, 1559325820936161. [PubMed: 32699536]
2. Li B, Shao H, Gao L, Li H, Sheng H and Zhu L, Drug Deliv, 2022, 29, 2130–2161. [PubMed: 35815678]
3. Liu SY and Wu YL, Expert Opin Investig Drugs, 2020, 29, 1355–1364.
4. Dirix LY, Takacs I, Jerusalem G, Nikolinakos P, Arkenau HT, Forero-Torres A, Boccia R, Lippman ME, Somer R, Smakal M, Emens LA, Hrinczenko B, Edenfield W, Gurtler J, von Heydebreck A, Grote HJ, Chin K and Hamilton EP, Breast Cancer Res Treat, 2018, 167, 671–686. [PubMed: 29063313]
5. Gong J, Chehrazi-Raffle A, Reddi S and Salgia R, J Immunother Cancer, 2018, 6, 8. [PubMed: 29357948]
6. Grenga I, Donahue RN, Lepone LM, Richards J and Schlom J, Clin Transl Immunology, 2016, 5, e83. [PubMed: 27350882]
7. Herbst RS, Giaccone G, de Marinis F, Reinmuth N, Vergnenegre A, Barrios CH, Morise M, Felip E, Andric Z, Geater S, Ozguroglu M, Zou W, Sandler A, Enquist I, Komatsubara K, Deng Y, Kuriki H, Wen X, McCleland M, Mocci S, Jassem J and Spigel DR, N Engl J Med, 2020, 383, 1328–1339. [PubMed: 32997907]
8. Upadhaya S, Neftelinov ST, Hodge J and Campbell J, Nat Rev Drug Discov, 2022, 21, 482–483. [PubMed: 35145263]
9. Majidpoor J and Mortezaee K, Clin Immunol, 2021, 226, 108707. [PubMed: 33662590]
10. Tang H, Wang Y, Chlewicki LK, Zhang Y, Guo J, Liang W, Wang J, Wang X and Fu YX, Cancer cell, 2016, 30, 500. [PubMed: 27622338]
11. Duan Q, Zhang H, Zheng J and Zhang L, Trends Cancer, 2020, 6, 605–618. [PubMed: 32610070]
12. Liu YT and Sun ZJ, Theranostics, 2021, 11, 5365–5386. [PubMed: 33859752]
13. Heinhuis KM, Ros W, Kok M, Steeghs N, Beijnen JH and Schellens JHM, Annals of oncology : official journal of the European Society for Medical Oncology / ESMO, 2019, 30, 219–235.
14. Kepp O, Zitvogel L and Kroemer G, Oncoimmunology, 2019, 8, e1637188. [PubMed: 31646079]
15. Hossain DMS, Javaid S, Cai M, Zhang C, Sawant A, Hinton M, Sathe M, Grein J, Blumenschein W, Pinheiro EM and Chackerian A, J Clin Invest, 2018, 128, 644–654. [PubMed: 29337311]
16. Bahadur KC R and Xu P, Advanced Materials, 2012, 24, 6479–6483. [PubMed: 23001909]
17. He H, Altomare D, Ozer U, Xu H, Creek K, Chen H and Xu P, Biomaterials Science, 2016, DOI: 10.1039/C5BM00325C.
18. Lelievre P, Sancey L, Coll JL, Deniaud A and Busser B, Cancers (Basel), 2020, 12. [PubMed: 33375055]
19. Zhu M, Yang M, Zhang J, Yin Y, Fan X, Zhang Y, Qin S, Zhang H and Yu F, Front Immunol, 2021, 12, 705361. [PubMed: 34489957]
20. Musetti S and Huang L, ACS nano, 2018, 12, 11740–11755. [PubMed: 30508378]

21. Oliveri V, Front Mol Biosci, 2022, 9, 841814. [PubMed: 35309510]
22. He F, Chang C, Liu B, Li Z, Li H, Cai N and Wang HH, Biomed Res Int, 2019, 2019, 4158415. [PubMed: 31218225]
23. Ruiz LM, Libedinsky A and Elorza AA, Front Mol Biosci, 2021, 8, 711227. [PubMed: 34504870]
24. da Silva DA, De Luca A, Squitti R, Rongioletti M, Rossi L, Machado CML and Cerchiaro G, Journal of inorganic biochemistry, 2022, 226, 111634. [PubMed: 34740035]
25. Wang F, Jiao P, Qi M, Frezza M, Dou QP and Yan B, Current medicinal chemistry, 2010, 17, 2685–2698. [PubMed: 20586723]
26. Nel AE, Madler L, Velegol D, Xia T, Hoek EM, Somasundaran P, Klaessig F, Castranova V and Thompson M, Nat Mater, 2009, 8, 543–557. [PubMed: 19525947]
27. Xia T, Kovochich M, Liong M, Zink JI and Nel AE, ACS nano, 2008, 2, 85–96. [PubMed: 19206551]
28. Aits S and Jaattela M, J Cell Sci, 2013, 126, 1905–1912. [PubMed: 23720375]
29. Liu WJ, Li ZH, Chen XC, Zhao XL, Zhong Z, Yang C, Wu HL, An N, Li WY and Liu HF, Scientific reports, 2017, 7, 8643. [PubMed: 28819100]
30. Wang F, Salvati A and Boya P, Open Biol, 2018, 8.
31. Ni YL, Chien PJ, Hsieh HC, Shen HT, Lee HT, Chen SM and Chang WW, International journal of molecular sciences, 2022, 23. [PubMed: 36613467]
32. Skrott Z, Mistrik M, Andersen KK, Friis S, Majera D, Gursky J, Ozdian T, Bartkova J, Turi Z, Moudry P, Kraus M, Michalova M, Vaclavkova J, Dzubak P, Vrobel I, Pouckova P, Sedlacek J, Miklovicova A, Kutt A, Li J, Mattova J, Driessen C, Dou QP, Olsen J, Hajduch M, Cvek B, Deshaies RJ and Bartek J, Nature, 2017, 552, 194–199. [PubMed: 29211715]
33. Allensworth JL, Evans MK, Bertucci F, Aldrich AJ, Festa RA, Finetti P, Ueno NT, Safi R, McDonnell DP, Thiele DJ, Van Laere S and Devi GR, Mol Oncol, 2015, 9, 1155–1168. [PubMed: 25769405]
34. Dang F, Nie L and Wei W, Cell death and differentiation, 2021, 28, 427–438. [PubMed: 33130827]
35. Chen X, Dou QP, Liu J and Tang D, Front Mol Biosci, 2021, 8, 649151. [PubMed: 33928122]
36. Ciechanover A and Schwartz AL, Proc Natl Acad Sci U S A, 1998, 95, 2727–2730. [PubMed: 9501156]
37. Tanaka K, Proc Jpn Acad Ser B Phys Biol Sci, 2009, 85, 12–36.
38. Latham MP, Sekhar A and Kay LE, Proc Natl Acad Sci U S A, 2014, 111, 5532–5537. [PubMed: 24706783]
39. Yim WW and Mizushima N, Cell Discov, 2020, 6, 6. [PubMed: 32047650]
40. Zhang J, Bu X, Wang H, Zhu Y, Geng Y, Nihira NT, Tan Y, Ci Y, Wu F, Dai X, Guo J, Huang YH, Fan C, Ren S, Sun Y, Freeman GJ, Sicinski P and Wei W, Nature, 2018, 553, 91–95. [PubMed: 29160310]
41. Gou Q, Dong C, Xu H, Khan B, Jin J, Liu Q, Shi J and Hou Y, Cell Death Dis, 2020, 11, 955. [PubMed: 33159034]
42. Li C, Wang X, Li X, Qiu K, Jiao F, Liu Y, Kong Q, Liu Y and Wu Y, Frontiers in cell and developmental biology, 2019, 7, 170. [PubMed: 31508418]
43. Ding WX, Ni HM, Gao W, Yoshimori T, Stolz DB, Ron D and Yin XM, Am J Pathol, 2007, 171, 513–524. [PubMed: 17620365]
44. Song W, Shen L, Wang Y, Liu Q, Goodwin TJ, Li J, Dorosheva O, Liu T, Liu R and Huang L, Nat Commun, 2018, 9, 2237. [PubMed: 29884866]
45. Clark PR and Menoret A, Cell Stress Chaperones, 2001, 6, 121–125. [PubMed: 11599573]
46. Fu X, Liu Z, Xiang L, Liu M, Zheng X, Wang J, Liu N, Gao H, Jiang A, Yang Y, Liang X, Ruan Z, Tian T and Yao Y, Cancer management and research, 2020, 12, 10939–10948. [PubMed: 33154673]
47. Jiang X, Wang J, Deng X, Xiong F, Ge J, Xiang B, Wu X, Ma J, Zhou M, Li X, Li Y, Li G, Xiong W, Guo C and Zeng Z, Mol Cancer, 2019, 18, 10. [PubMed: 30646912]

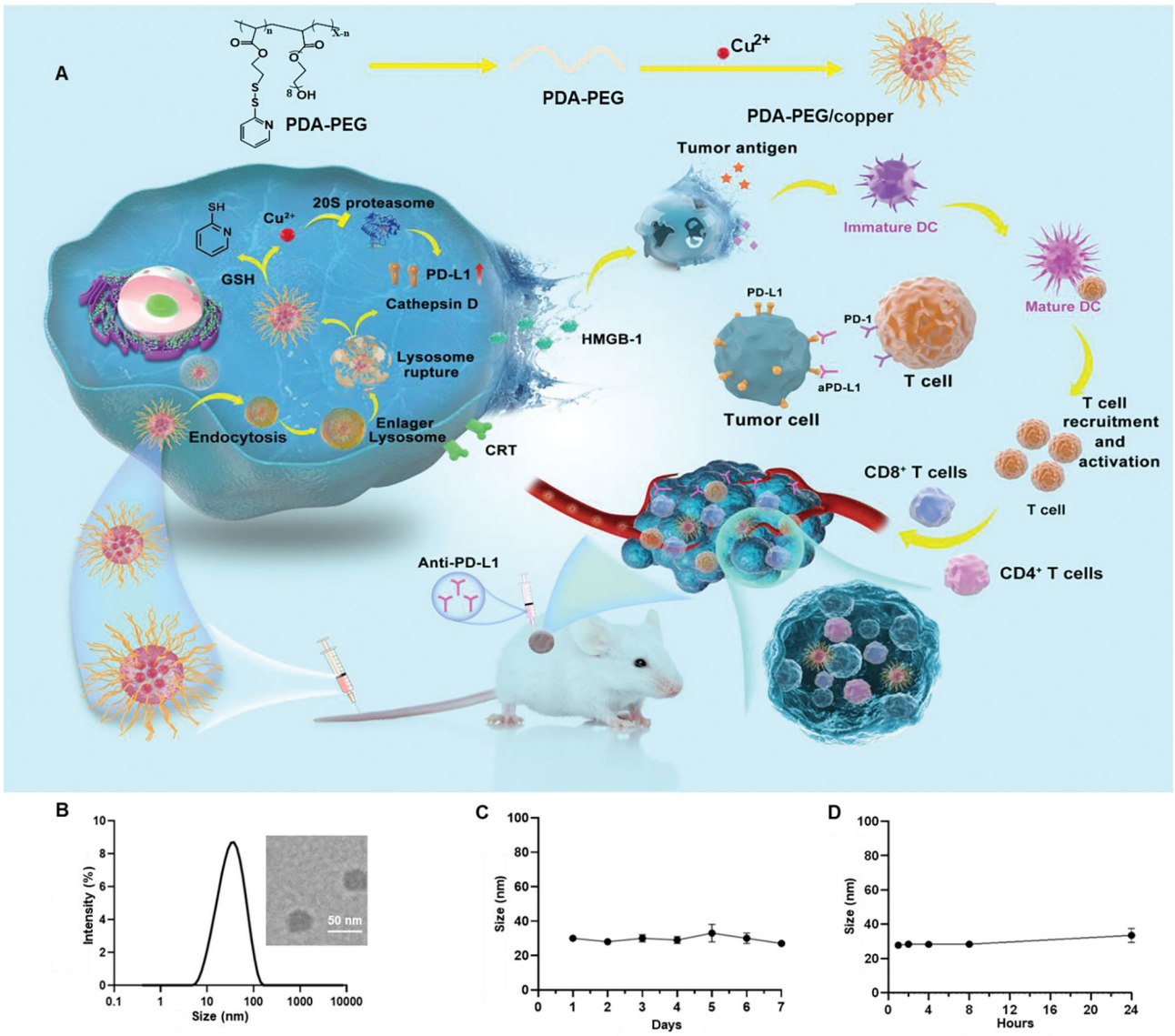

Fig. 1.

The proposed action of Poly/Cu nanocomplex and its characterization. (A) Schematic illustration of the preparation process of Poly/Cu nanocomplex, mechanism of it killing 4T1 cells and combined with aPD-L1 for the combination therapy. (B) The DLS size of Poly/Cu nanocomplexes was determined by Nano ZS Zetasizer and TEM image of Poly/Cu nanocomplexes (insert). (C) The size change curve of Poly/Cu nanocomplexes in PBS buffer was determined for 7 days. (D) The size change curve of Poly/Cu nanocomplexes in 10% FBS at 37°C.

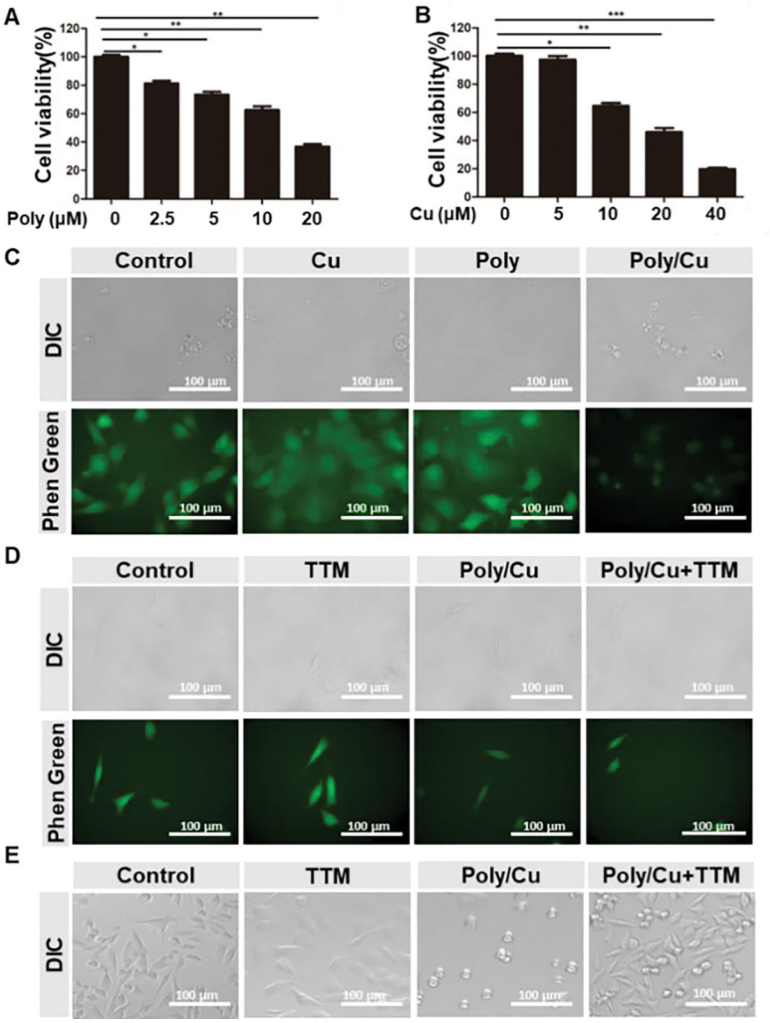

Fig. 2.

Poly/Cu delivers copper ions into 4T1 cells. (A) Different concentrations of polymer combined with 10 μM $CuCl_2$ were incubated with 4T1 cells for 48 h, and the cell viability was determined by MTT assay. Data are shown as mean ± SD. * $p < 0.05$, ** $p < 0.01$, *** $p < 0.001$, n=5. (B) 10 μM polymer combined with different concentrations of $CuCl_2$ were incubated with 4T1 cells for 48 h, and the cell viability was determined by MTT assay. Data are shown as means ± SD. * $p < 0.05$, ** $p < 0.01$, *** $p < 0.001$, n=5. (C) 10 μM $CuCl_2$, 20 μM polymer, and their combination were incubated with 4T1 cells for 6 h, and the old medium was replaced with a fresh medium containing Phen Green™ FL Diacetate dye. The copper concentration in the 4T1 cells was detected by confocal microscopy. (D) 20 μM TTM, 20 μM polymer/ 10 μM $CuCl_2$, and their combination were incubated with 4T1 cells for 6 h, and the old medium was replaced with a fresh medium containing Phen Green™ FL Diacetate dye. The copper concentration in the 4T1 cells was detected by confocal microscopy. (E) 20 μM TTM, 20 μM polymer/10 μM $CuCl_2$, and their combination were incubated with 4T1 cells for 48 h. The cells' morphology was determined by a light microscope.

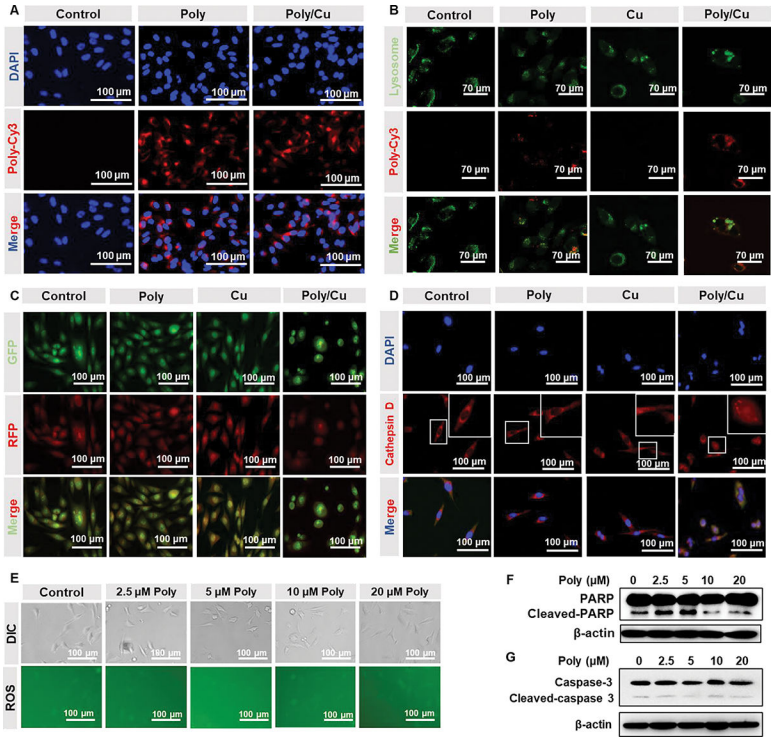

Fig. 3.

Poly/Cu induces lysosomal cell death. (A) 4T1 cells were treated with 20 μM Poly-Cy3 or 20 μM Poly-Cy3/10 μM $CuCl_2$ for 4 h. The uptake of PDA-PEG was detected by confocal microscopy. (B) 4T1 cells were incubated with 20 μM Poly-Cy3, 10 μM $CuCl_2$, and their combination for 12 h. The lysosomes of the 4T1 cells were labeled with Lysotracker (green) and detected by confocal microscopy. (C) 4T1 cells were incubated with 20 μM Polymer, 10 μM $CuCl_2$, and their combination for 24 h. The permeability of lysosomes was determined by the confocal with the help of Acridine orange staining. (D) 4T1 cells were treated with indicated drugs for 24 h, and the distribution of cathepsin D was detected by immunofluorescent staining. (E) Different concentrations of Polymer combined with 10 μM $CuCl_2$ were incubated with 4T1 cells for 12 h, ROS in the 4T1 cells was investigated with a ROS detection kit. Different concentrations of Polymer combined with 10 μM $CuCl_2$ were incubated with 4T1 cells for 48 h, the cleaved-PARP (F) and cleaved-caspase-3 (G) protein expressions were analyzed by western blot.

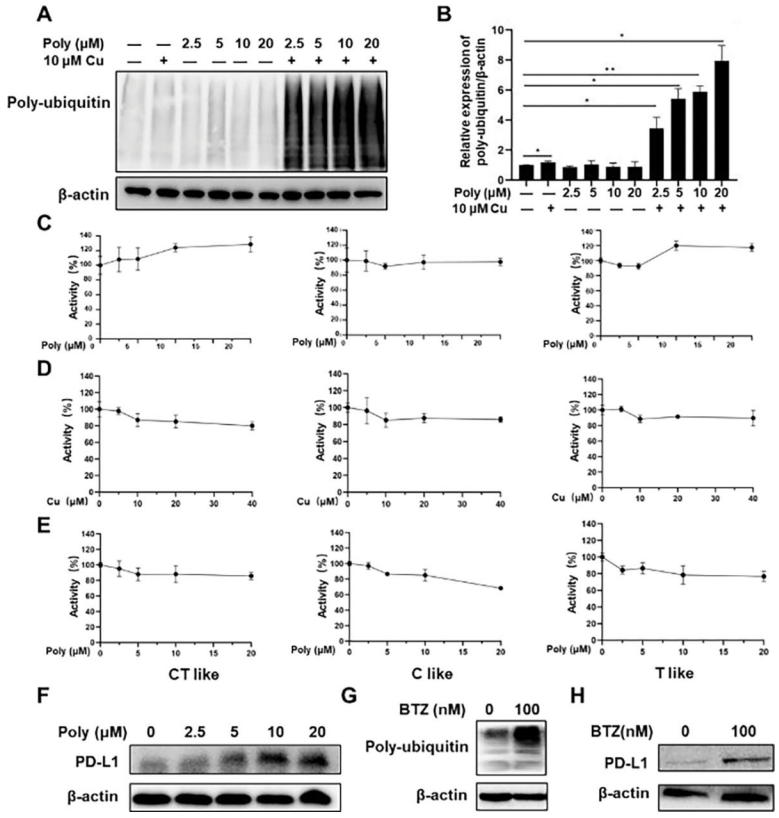

Fig. 4.

Poly/Cu inhibits the function of the proteasome in 4T1 cells and prevents the degradation of PD-L1. (A) 4T1 cells were treated with different concentrations of Polymer, 10 μM $CuCl_2$, and their combination for 48 h, the poly-ubiquitin protein expression was evaluated by western blot. (B) Quantitative expression of Poly-ubiquitin after the treatments in (A). Data are shown as means ± SD. * $p < 0.05$, n=3. The 4T1 cells were treated with (C) Polymer alone, (D) $CuCl_2$ alone, and (E) different concentrations of Polymer combined with 10 μM $CuCl_2$ for 48 h, the 20 S proteasome was isolated from 4T1 cells, and the activity of 20S was analyzed with different substrates. (F) 4T1 cells were treated with different concentrations of Poly combined with 10 μM $CuCl_2$ for 48 h, and the PD-L1 protein expression was evaluated by western blot. 4T1 cells were incubated with BTZ 100 nM for 48 h, and Poly-ubiquitin (G) and PD-L1(H) protein expression were evaluated by western blot.

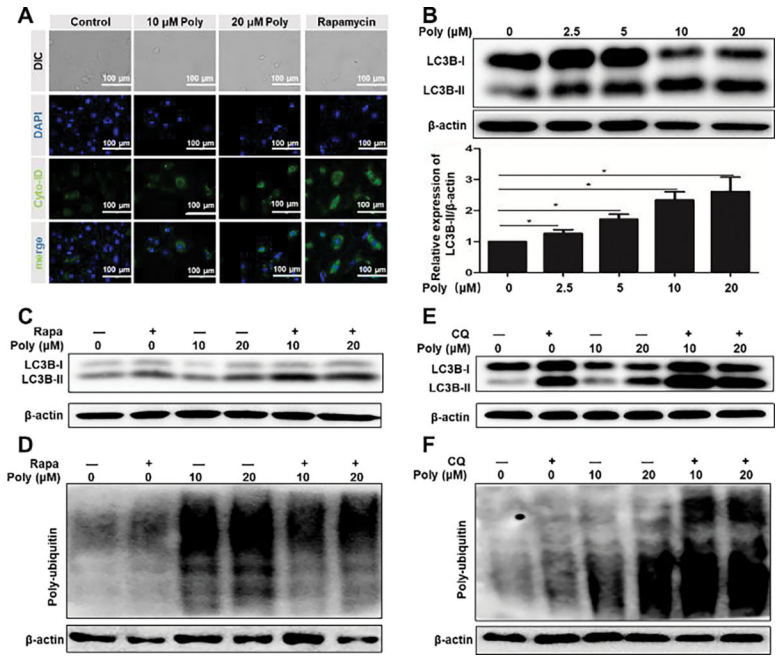

Fig. 5.

Poly/Cu inhibits autophagy. (A) 4T1 cells were treated with different concentrations of Polymer combined with 10 μM $CuCl_2$ and 500 nM Rapamycin for 24 h. The cell autophagy was detected with the Cyto-ID kit. (B) 4T1 cells were treated with different concentrations of Polymer/10 μM $CuCl_2$ for 48 h, and LC3B-II protein expression was analyzed by western blot. Data were represented as mean ± SD (*P < 0.05). 4T1 cells were treated with 31.25 nM Rapamycin combined with different concentrations of Polymer/10 μM $CuCl_2$ for 24 h, the expressions of LC3B-II (C) poly-ubiquitin (D) were determined by western blot. 4T1 cells were treated with 3.125 μM CQ combined with different concentrations of Poly/10 μM Cu for 24 h, and the expressions of LC3B-II (E) poly-ubiquitin (F) were determined by western blot.

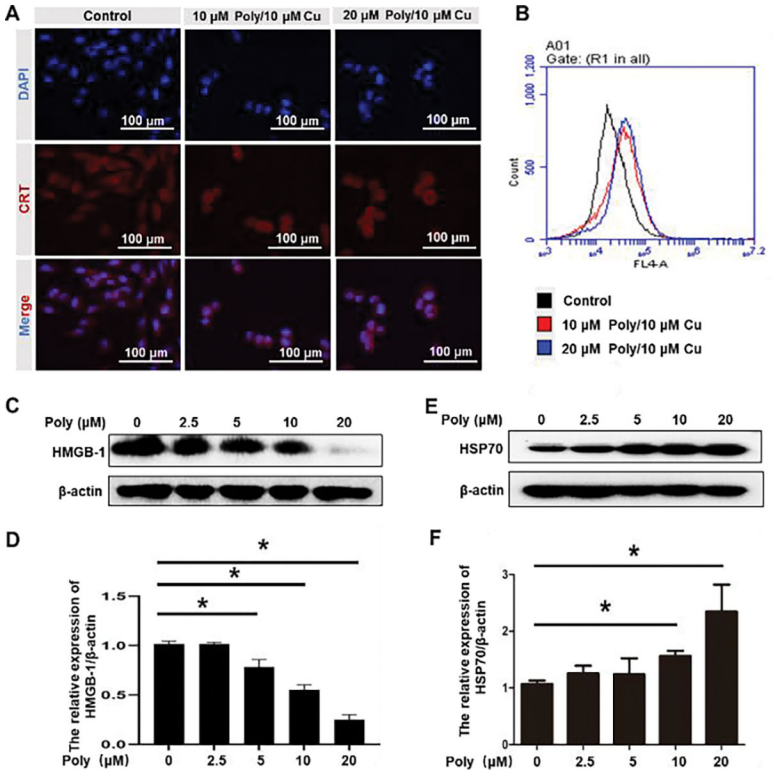

Fig.6.

Poly/Cu induces ICD in 4T1 cells. 4T1 cells were treated with 10 μM Polymer/10 μM $CuCl_2$, and 20 μM Polymer/10 μM $CuCl_2$ for 48 h, the expression of CRT on 4T1 cell membrane was investigated by immunofluorescent staining (A) and flow cytometry (B). 4T1 cells were treated with different concentrations of Polymer/10 μM Cu for 48 h. HMGB-1 (C) and HSP70 (D) protein expression were analyzed by western blot. Quantitative analysis of the expression of LC3B-II (d) and HSP 70 (F) in (C) and (E), respectively. Data were represented as mean ± SD (*$P < 0.05$).

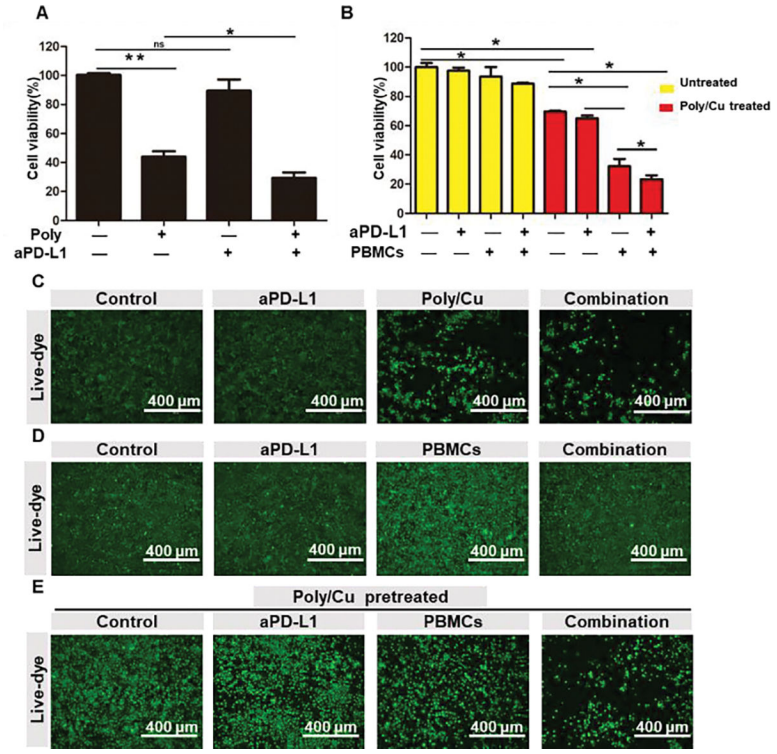

Fig. 7.

aPD-L1 boosts the cell-killing effect of Poly/Cu *in vitro*. (A) 4T1 cells were treated with 20 μM Polymer/ 10 μM $CuCl_2$ combined with aPD-L1 (50 μg/ml) for 48 h, the cell viability was determined by MTT. (C) The cell density of different treatment was recorded by microscope with the help of live dye. 4T1 cells were pretreated with (E) or without (D) 20 μM Polymer/ 10 μM $CuCl_2$ for 48 h, and then treated with aPD-L1 (50 μg/ml), PBMCs (E/T=30) or their combination for 5 days. Cell viability was evaluated by MTT assay (B), or the cell density of different treatments was determined by microscope with the help of live dye (D) and (E).

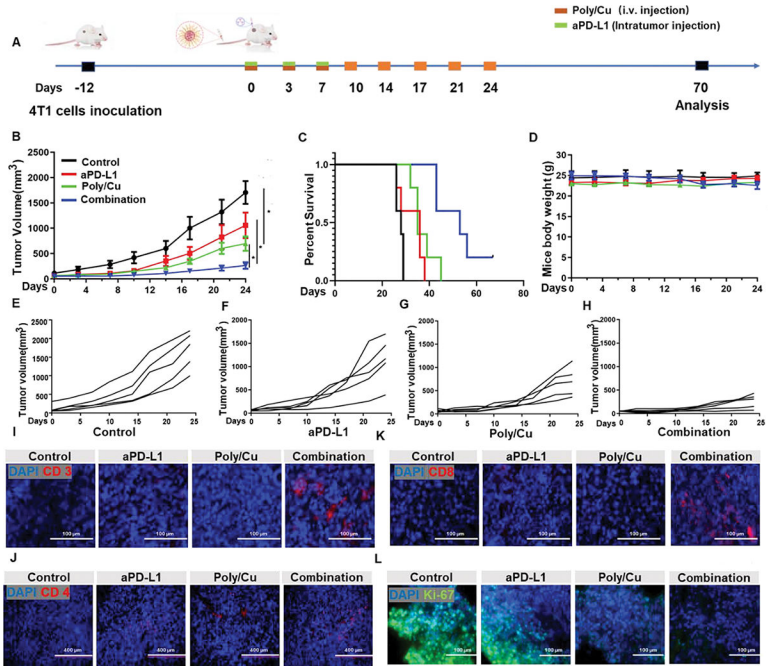

Fig. 8.

In vivo antitumor effect of the combinatory treatment. (A) The schedule of tumor inoculation, drug administration, and therapy evaluation. (B) The tumor volume change curve during treatment. (C) The survival time of the animals in different treatment groups. (D) The body weight change curve during treatment. The tumor growth curves in control (E), aPDL1 (F), Poly/Cu (G), and combinatory treatment (H) groups. The infiltration of $CD3^+$ cells (I), $CD4^+$ cells (J), $CD8^+$ cells (K), and proliferating cells (L) within tumor tissue from different treatment groups detected with anti-CD3, anti-CD4, anti-CD8, and anti-Ki-67 antibodies, respectively.